

Cambridge University Press

978-1-107-41108-1 - Materials Research Society Symposia Proceedings: Volume 93:

Materials Modification and Growth Using Ion Beams

Editors: Ursula Gibson, Alice E. White and Peter P. Pronko

Excerpt

[More information](#)

PART I

**Fundamental Ion-Solid
Interactions (I)**

Cambridge University Press

978-1-107-41108-1 - Materials Research Society Symposia Proceedings: Volume 93:

Materials Modification and Growth Using Ion Beams

Editors: Ursula Gibson, Alice E. White and Peter P. Pronko

Excerpt

[More information](#)

Cambridge University Press

978-1-107-41108-1 - Materials Research Society Symposia Proceedings: Volume 93:

Materials Modification and Growth Using Ion Beams

Editors: Ursula Gibson, Alice E. White and Peter P. Pronko

Excerpt

[More information](#)

3

Indium Ion Doping During Si Molecular Beam Epitaxy

N. Hirashita,* J.-P. Noel,* A. Rockett,* L. Markert,* J.E. Greene,* M.A. Hasan,** J. Knall,** W.-X. Ni,** and J.-E. Sundgren**

* Department of Materials Science, the Coordinated Science Laboratory, and the Materials Research Laboratory, University of Illinois, Urbana, Illinois, 61801, USA

** Department of Physics, Linköping University, S-58183 Linköping, Sweden

ABSTRACT

A single-grid UHV-compatible ion source was used to provide partially-ionized accelerated In^+ dopant beams during Si growth by molecular beam epitaxy (MBE). Indium incorporation probabilities in 800 °C MBE Si(100), as measured by secondary ion mass spectrometry, ranged from $< 10^{-5}$ (the detection limit) for thermal In to values of 0.02–0.7 for In^+ acceleration energies E_{In} between 50 and 400 eV. Temperature-dependent Hall-effect and resistivity measurements were carried out on Si films grown at 800 °C with $E_{\text{In}} = 200$ eV. Indium was incorporated substitutionally in electrically active sites over the entire concentration range examined, 10^{16} – 10^{19} cm^{-3} , with an acceptor level ionization energy of 165 meV. The 111 meV level associated with In-C complexes and the 18 meV "supershallo" level reported for In ion-implanted Si were not observed. Room-temperature hole mobilities μ were higher than both annealed In-ion-implanted Si and Irvin's values for bulk Si. Phonon scattering was found to dominate at temperatures between 100 and 330 K and μ varied as $T^{-2.2}$.

1. Introduction

Molecular beam epitaxy (MBE) has become a well-established technique for the growth of epitaxial Si films. However, many of the common dopants used in bulk Si technology present problems during MBE growth due to low incorporation probabilities and/or pronounced surface segregation making control over both dopant concentrations and depth distributions difficult over a wide range in growth conditions.⁽¹⁾ Ota⁽²⁾ was one of the first to show that dopant incorporation probabilities σ could be increased by several orders of magnitude using accelerated-ion doping during deposition. σ , which was undetectable for thermal As in MBE Si at growth temperatures $T_s > 600$ °C, was found to be nearly unity for acceleration energies E_{As} between 400 and 800 eV at T_s up to 800 °C and decreased at higher temperatures to 0.08–0.17 (depending upon E_{As}) at 1050 °C. The experimental results were explained by Bajor and Greene⁽³⁾ using a model which accounted for both trapping (i.e., low-energy implantation) and the effect of implantation on surface-segregation kinetics.

Indium is a deep-level acceptor in Si which is of interest for infrared devices. Unfortunately, σ_{In} for thermal In in MBE Si(100) is $< 10^{-5}$ for $T_s > 450$ °C. Even with charged particle bombardment during Si growth from an electrostatically-focused electron beam evaporator, σ_{In} ranges from ~ 0.1 at 550 °C to $< 10^{-4}$ at $T_s > 750$ °C.⁽⁴⁾ These low and strongly temperature-dependent incorporation probabilities combined with a high SIMS sensitivity make In a good candidate for a model dopant in accelerated-beam doping studies. Rockett et al.⁽⁵⁾ have recently observed several orders of magnitude increases in σ_{In} for accelerated- In^+ in MBE Si with $E_{\text{In}} = 100$ eV. Accelerated-ion doping was also shown to result in abrupt doping profiles in Si:In modulation doped structures.

In this paper, we present the results of an investigation of the incorporation probability of accelerated- In^+ in Si and the electrical characteristics of MBE Si(100) films doped with 200 eV In^+ ions during deposition. The films were grown at 800 °C using a magnetically-focused electron gun to provide the Si flux and a single-grid ion source to provide the accelerated- In^+ ions. Steady-state In concentrations C_{In} measured by secondary ion mass spectrometry (SIMS), using known standards, agreed very well with acceptor-level concentration values obtained from Hall measurements. σ_{In^+} was found to range from 0.02 to 0.7 for acceleration energies between 50 and 400 eV.

An analysis of the carrier concentration p vs. inverse temperature for films grown at $E_{\text{In}} = 200$ eV showed that In doping resulted in an acceptor level at $\epsilon_{\text{In}} = 165$ meV above the valence-band edge consistent with results for bulk In-doped Si.⁽⁶⁾ No evidence was found for the presence of the 111 meV level associated with the In-C complex⁽⁷⁾ or the supershallo level at 18 meV⁽⁸⁾ which has been reported in In ion-implanted Si. Room temperature hole mobilities were higher than previously reported values for annealed In-ion-implanted Si.⁽⁹⁾ From the entire set of results, we conclude that 200 eV accelerated-In species occupy normal substitutional lattice sites in Si films

grown at $T_s = 800^\circ\text{C}$ (even for C_{In} well above the maximum reported solid solubility limit)⁽¹⁰⁾ with no evidence of residual lattice damage. Increasing E_{In} to 500 eV while decreasing T_s to 600°C did, however, result in both a loss of In substitutionality and a decrease in the carrier mobility.

II. Experimental Procedure

All films were grown in a Vacuum Generators VG-80 MBE system with a base pressure of 5×10^{-11} Torr. The growth system, as well as substrate preparation and film deposition conditions, have been described in detail previously^(5,11) and only a few essential details will be discussed here. The films were deposited on n-type Si (100) wafers (resistivity = 7–13 or 1000–3000 Ωcm), that were chemically cleaned through an oxide etch/regrowth procedure. Final cleaning consisted of *in-situ* oxide removal by heating to 1000°C for 30 s. This substrate treatment resulted in Si surfaces free of contaminants detectable by Auger electron spectroscopy. Sharp (2x1) reflection high-energy electron diffraction (RHEED) and low-energy electron diffraction (LEED) patterns were obtained.

The Si flux was provided by a magnetically-focused electron-beam evaporator and the In dopant flux by either a conventional effusion cell or by a single-grid hot-cathode low-energy ion source similar to that of Rockett et al.⁽¹²⁾ The Si flux was maintained at $1 \times 10^{15} \text{ cm}^{-2}\text{s}^{-1}$ and was monitored using both a quartz-crystal oscillator and a nude ion gauge. Total film thicknesses, measured with a microstylus, ranged from 1 to 5 μm and deposition, except where noted, was carried out at 800°C . The In^+ ion flux, which ranged from $\sim 10^9$ to $10^{13} \text{ cm}^{-2}\text{s}^{-1}$, was measured using a Faraday cup which could be rotated to a position 2 cm below the substrate.

Indium concentrations C_{In} in as-deposited films were determined by secondary ion mass spectroscopy (SIMS), referenced to In-ion-implanted bulk Si(100) standards, using a Cameca IMS 3F ion microprobe operated with a 5.5 kV, 1 μA , O_2^+ ion beam. The SIMS detection limit for In in Si was $\sim 5 \times 10^{14} \text{ cm}^{-3}$ and C_{In} in the present films ranged from $\sim 10^{16}$ – 10^{19} cm^{-3} . Electrical properties of the In-doped Si films were investigated by means of temperature-dependent Hall and resistivity measurements carried out between 77 and 330 K. The films were electrically isolated from the substrates via p-n junctions and were photolithographically patterned in van der Pauw,⁽¹³⁾ mesa structures. The contacts were evaporated Al pads which for lightly doped films were sintered at 500°C for 10 min. Gold electrical leads were then wire-bonded to the contact pads.

III. Experimental Results and Discussion

A. Indium Incorporation

The incorporation probability σ_{In} of thermal In was found to be less than 10^{-5} at $T_s = 800^\circ\text{C}$ using a magnetically-focused electron-beam evaporator to provide the Si flux. The low incorporation probability results from a strong tendency for In adatoms to follow the advancing film surface and the relatively high desorption rate of In at elevated deposition temperatures. The In segregation rate at the Si growth front was extremely rapid since it involved primarily surface diffusion. The steady-state In surface coverage θ_{In} was, depending upon J_{In} , large enough to cause the surface reconstruction to change from the initial Si(2x1) to In-stabilized (3x4), corresponding to $\theta_{\text{In}} > 0.1$ monolayer (ML), or even to In(3x4) with (310) facets at $\theta_{\text{In}} > 0.7$ ML, without any detectable In incorporation in the bulk film. In order to obtain σ_{In} values larger than 10^{-5} , T_s had to be reduced to $\leq 450^\circ\text{C}$ resulting in poor crystalline quality.

The use of partially-ionized low-energy accelerated In^+ ion beams was, however, found to greatly enhance the In incorporation probability. Figure 1 shows the In^+ ion incorporation probability σ_{In^+} as a function of the acceleration energy E_{In} from 50 to 400 eV for Si(100) films grown at 800°C . Since σ_{In} for thermal In was negligible at this temperature, the incorporation probabilities of the accelerated ions were determined directly from the measured ion currents. σ_{In^+} was nearly unity at $E_{\text{In}} = 400$ eV and decreased slowly to 0.2 at 100 eV. At lower ion energies, σ_{In^+} decreased more rapidly but was still 0.02, more than three orders of magnitude larger than the value for thermal In, at $E_{\text{In}} = 50$ eV. These large enhancements in the incorporation probability can be understood in terms of low-energy ion implantation at the higher acceleration energies and the creation of immobile preferential adsorption sites⁽¹⁴⁾ at lower E_{In} values. Both of these effects decrease the steady-state In surface coverage and hence the In desorption rate. They also result in abrupt doping profiles as can be seen in Figure 2 which shows a SIMS profile from a 100 eV In^+ modulation-doped film. The widths of the interfaces separating doped and undoped regions in the film are of the order of the depth resolution of the SIMS measurement. The broadening of the lower interface of the 935°C layer was due primarily to bulk diffusion.

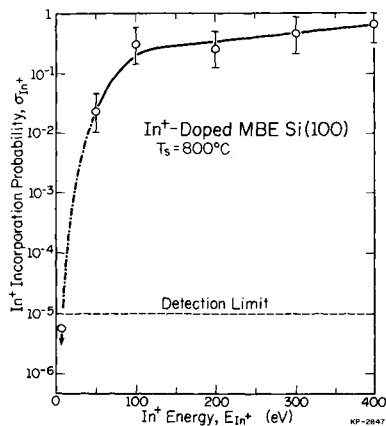


Figure 1. Incorporation probability σ_{In^+} of accelerated In ions in Si(100) during MBE growth at 800 °C as a function of ion energy E_{In^+} .

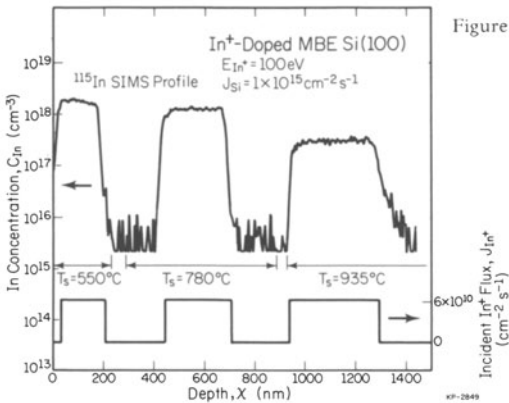


Figure 2. SIMS doping profile through a multilayer MBE Si(100) film with layers grown at temperatures between 550 and 935 °C and doped with 100 eV accelerated In⁺ ions according to the schedule shown in the insert.

B. Electrical Properties of In⁺ Ion-Doped Si

All films were found to be p-type. The hole concentration, p , was determined from the measured Hall coefficient, R_H , using the relation⁽¹⁵⁾ $p = r/qR_H$, where q is the electron charge and r is the Hall scattering factor defined as the ratio of the Hall mobility to the conductivity mobility. A convenient treatment of hole transport assumes a scattering factor of unity, but this has been shown to cause an overestimation of the In concentration in bulk Si.⁽¹⁶⁾ In our study, a temperature independent value of $r = 0.77$, from Parker et al.,⁽¹⁷⁾ was used. We also assumed that r was independent of the In concentration consistent with the weak functional dependence reported by Lin et al.⁽¹⁸⁾

Figure 3 shows typical variations of the hole concentration with reciprocal temperature. At higher temperatures, the In acceptor (whose activation energy ϵ_{In} is too deep to allow complete ionization as evidenced by the lack of an "exhaustion" region) dominates the carrier concentration. The slope in the $\ln(p)$ vs. T^{-1} plot corresponds to $\sim 0.5\epsilon_{In}$ (i.e., the Fermi level ϵ_F is approximately midway between the In acceptor level and the top of the valence band) indicating that the concentration of any unintentional donors is low. The curvature in the $\ln(p)$ vs. T^{-1} plot at low temperatures, however, indicates the presence of an unintentional shallow acceptor.

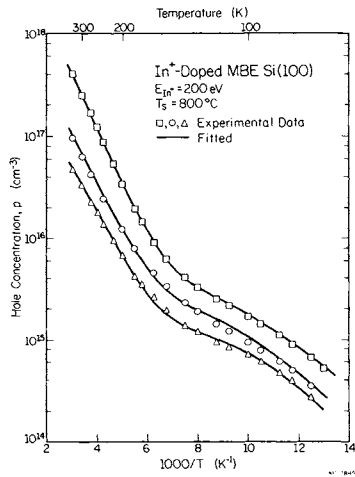
The solid lines in Figure 3 represent calculated values obtained from a model including two independent acceptors with background donor compensation. Since In is a deep acceptor, the non-degeneracy criterion $|\epsilon_F - \epsilon_v| \geq 3.5kT$,⁽¹⁹⁾ where ϵ_v is the energy corresponding to the top of the

valence band, was satisfied. All three valence bands were accounted for in the density-of-states effective mass⁽²⁰⁾ and the hole degeneracy factor. Equally good fits were obtained for all samples ($1.4 \times 10^{16} \text{ cm}^{-3} \leq N_{\text{In}} \leq 9.6 \times 10^{18} \text{ cm}^{-3}$). A value of $N_d = 4 \times 10^{14} \text{ cm}^{-3}$ was assumed for the background donor density comparable to values reported in other MBE Si films.⁽²¹⁾ The best-fit values obtained for ϵ_{In} , $165 \pm 10 \text{ meV}$, agreed well with previously published Hall-effect measurements carried out on bulk Si:In⁽⁶⁾ but were slightly deeper than the optically determined results⁽²²⁾ of 156 meV . No evidence of a reduction of the In acceptor level due to screening was observed over the concentration range investigated here.

The In acceptor concentrations N_{In} determined from analysis of the Hall data were found to be in good agreement with the chemical concentrations C_{In} determined by SIMS analyses as shown in Figure 4. This indicates that In is incorporated at electrically-active (substitutional) sites in concentrations up to $\sim 10^{19} \text{ cm}^{-3}$ without significant clustering or precipitation. The maximum reported measured In solid solubilities in Si range from $\sim 5 \times 10^{16}$ (9) to $4 \times 10^{17} \text{ cm}^{-3}$.⁽²³⁾ Post-annealing of the $N_{\text{In}} \simeq 10^{19} \text{ cm}^{-3}$ sample at 1000°C for 1 h showed that it was indeed metastable as some excess In came out of solution and the In acceptor concentration decreased to $2 \times 10^{18} \text{ cm}^{-3}$.

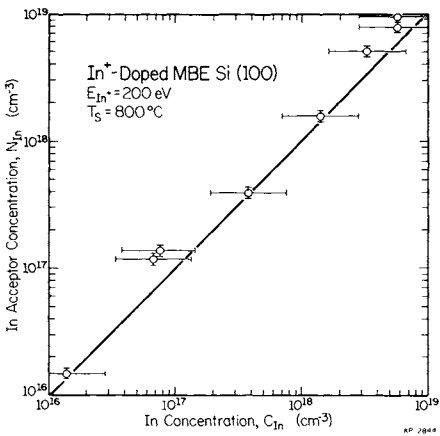
The concentration of unintentional shallow acceptors was found to be $\leq 1\%$ of the In concentration with an activation energy of $56 \pm 4 \text{ meV}$. We believe that the shallow acceptor is Al, a common impurity in In. The same activation energy was measured in samples that were

Figure 3.



Temperature dependence of the hole concentration p for MBE: Si(100) films grown at 800°C and doped with 200 eV In^+ ions.

Figure 4.



In acceptor concentration N_{In} , determined from Hall data, vs In concentration C_{In} obtained from SIMS analyses of MBE: Si(100) films grown at 800°C and doped with 200 eV In^+ ions.

intentionally doped with Al. No evidence was found for the presence of the supershallow 18 meV level reported in In ion-implanted Si. The 111 meV level associated with In-C complexes⁽⁷⁾ was also not observed except immediately after cleaning the ultra-high-purity graphite grid used in the In ion source where the first film showed a concentration of $\leq 5 \times 10^{15} \text{ cm}^{-3}$. However, as the grid became covered with a thin layer of In, this level disappeared.

Cambridge University Press

978-1-107-41108-1 - Materials Research Society Symposia Proceedings: Volume 93:

Materials Modification and Growth Using Ion Beams

Editors: Ursula Gibson, Alice E. White and Peter P. Pronko

Excerpt

[More information](#)

7

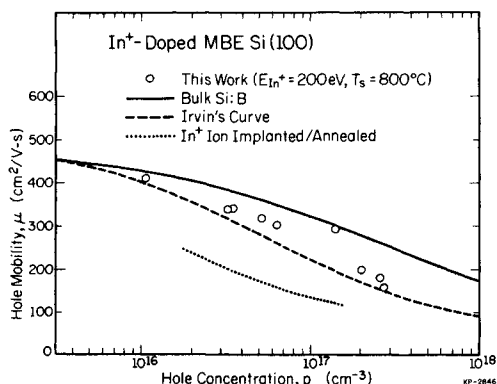


Figure 5. Conductivity mobility μ vs hole concentration p at 300 K in MBE Si(100) films grown at 800 °C and doped with 200 eV In^+ ions.

Hole conductivity mobilities μ measured at 300 K are shown as a function of hole concentration in Figure 5. The well-established Irvin mobility curve⁽²⁴⁾ and the recent theoretical mobility fit⁽²⁵⁾ to the best published bulk Si:B data⁽²⁶⁾ are also shown for comparison together with results from annealed In-ion-implanted Si.⁽⁹⁾ The present mobilities were found to be higher than both Irvin's curve and the mobilities of ion-implanted and annealed Si but lower than the best bulk Si:B data. The latter result is not, however, an indication of reduced crystalline quality since neutral-impurity scattering is higher for In than for B and the amount of ionized-impurity scattering due to background donors is larger in MBE films than in ultra-high purity bulk Si:B. The measured temperature dependence of the hole mobilities in present films was found to follow a $T^{-2.2}$ relationship as expected for phonon scattering.⁽²⁵⁾

Considering the entire set of results presented above, we conclude that 200 eV accelerated-In species exhibit an incorporation probability more than 5 orders of magnitude higher than thermal In and occupy normal lattice sites with no evidence of residual lattice damage in Si films grown at 800 °C. In fact, substitutionality was maintained even at In concentrations well above reported equilibrium solid-solubility limits. Residual damage was observable only in films grown with higher acceleration energies at lower deposition temperatures. For example, at $E_i = 500$ eV and $T_S = 600$ °C, $N_{\text{In}}/C_{\text{In}}$ was 0.03 and the mobility was reduced by $\sim 30\%$.

ACKNOWLEDGEMENTS

The authors gratefully acknowledge the financial support of the Semiconductor Research Corporation, the Joint Services Electronics Program, and the Swedish National Science Research Council (NFR) during the course of this research. The SIMS analyses were carried out at the University of Illinois Center for Microanalysis of Materials which is partially supported by the Department of Energy.

REFERENCES

1. J.E. Greene, S.A. Barnett, A. Rockett, and G. Bajor, *Appl. Surf. Sci.* 22/23, 520 (1985).
2. Y. Ota, *J. Appl. Phys.* 51, 1102 (1980).
3. G. Bajor and J.E. Greene, *J. Appl. Phys.* 54, 1579 (1983).
4. M.-A. Hasan, J. Knall, S.A. Barnett, A. Rockett, J.-E. Sundgren, and J.E. Greene, unpublished.
5. A. Rockett, J. Knall, M.A. Hasan, J.-E. Sundgren, S.A. Barnett, and J.E. Greene, *J. Vac. Sci. Technol.* A4, 900 (1986).
6. R.N. Thomas, T.T. Braggins, H.M. Hobgood, and W.J. Takei, *J. Appl. Phys.* 49, 2811 (1978).
7. R. Baron, J.P. Baukus, S.D. Allen, T.C. McGill, M.H. Young, H. Kimura, H.V. Winston, and O.J. Marsh, *Appl. Phys. Lett.* 34, 257 (1979).

Cambridge University Press

978-1-107-41108-1 - Materials Research Society Symposia Proceedings: Volume 93:

Materials Modification and Growth Using Ion Beams

Editors: Ursula Gibson, Alice E. White and Peter P. Pronko

Excerpt

[More information](#)

8. G.F. Cerofolini, G.U. Pignatelli, E. Mazzega, and G. Ottavini, *J. Appl. Phys.* **58**, 2204 (1985).
9. G.F. Cerofolini, G. Ferla, G.U. Pignatelli, and F. Riva, *Thin Solid Films* **101**, 2204 (1985).
10. Landolt-Börnstein, *Numerical Data and Functional Relationship in Science and Technology, Group B, Vol. 17, Semiconductors*, eds. O. Madelung, M. Schulz and H. Weiss (Springer, Berlin, 1984).
11. J. Knall, J.-E. Sundgren, G.V. Hansson, and J.E. Greene, *Surf. Sci.* **166**, 512 (1986).
12. A. Rockett, S.A. Barnett, and J.E. Greene, *J. Vac. Sci. Technol.* **B2**, 306 (1984).
13. L.J. van der Pauw, *Philips Res. Repts.* **13**, 1 (1958).
14. S.A. Barnett, H.F. Winters, and J.E. Greene, *Surf. Sci.*, in press.
15. S.M. Sze, *Physics of Semiconductor Devices*, 2nd ed. (John Wiley and Sons 1981).
16. D.K. Schroder, T.T. Braggins, and H.M. Hobgood, *J. Appl. Phys.* **49**, 5256 (1978).
17. G.J. Parker, S.D. Brotherton, I. Gale, and A. Gill, *J. Appl. Phys.* **54**, 3926 (1983).
18. J.F. Lin, S.S. Li, L.C. Linares, and K.W. Teng, *Solid State Electronics* **24**, 827 (1981).
19. J.S. Blakemore, *Semiconductor Statistics* (Pergamon, Oxford, 1962).
20. J.E. Lang, F.L. Madarasz, and P.M. Hemenger, *J. Appl. Phys.* **54**, 3612 (1983).
21. R.A.A. Kubiak, W.Y. Leong, and E.H.C. Parker, *J. Vac. Sci. Technol.* **B3**, 592 (1985).
22. A. Onton, P. Fisher, and A.K. Ramdas, *Phys. Rev.* **163**, 686 (1967).
23. G. Backenstoss, *Phys. Rev.* **108**, 1416 (1957).
24. S.M. Sze and J.C. Irvin, *Solid-State Electronics* **11**, 599 (1968); and D.M. Caughey and R.E. Thomas, *Proc. IEEE* **55**, 2192 (1967).
25. S.S. Li, *Solid-State Electronics* **21**, 1109 (1978).
26. W.R. Thurber, R.L. Mattis, Y.M. Liu, and J.J. Fillibeau, *J. Electrochem. Soc.* **127**, 2291 (1980).

Cambridge University Press

978-1-107-41108-1 - Materials Research Society Symposia Proceedings: Volume 93:
Materials Modification and Growth Using Ion Beams

Editors: Ursula Gibson, Alice E. White and Peter P. Pronko

Excerpt

[More information](#)

9

ION IMPLANTATION AND ANNEALING OF SrTiO_3 AND CaTiO_3 [†]

C.W. WHITE*, L.A. BOATNER*, J. RANKIN**, AND M.J. AZIZ***

* Oak Ridge National Laboratory, Oak Ridge, TN 37831

** Massachusetts Institute of Technology, Cambridge, MA 02139

*** Division of Applied Sciences, Harvard University, Cambridge, MA 02138

ABSTRACT

Ion implantation damage and thermal annealing results are presented for single crystals of SrTiO_3 and CaTiO_3 . The near-surface region of both of these materials can be made amorphous by low doses ($\sim 10^{15}/\text{cm}^2$) of heavy ions (Pb at 540 keV). During annealing, the amorphous implanted region crystallizes epitaxially on the underlying single-crystal substrate. The kinetics of this solid-phase epitaxial recrystallization process have been measured by employing ion channeling techniques.

INTRODUCTION

Ion implantation techniques are currently being extensively investigated as methods for altering the near surface optical, electrical, or mechanical properties of insulating materials.¹⁻⁶ Ion implantation processes generate extensive damage in the near-surface region of such materials; for a number of important applications it will be necessary to anneal the implanted insulating materials in order to remove or minimize the implantation-induced disorder. In contrast to the case of either Si or Ge, there are only a few reported investigations of the effects of damage production associated with the implantation of insulating materials or their subsequent behavior during thermal annealing processes. Ion implantation is currently being used to modify the near-surface properties of a wide range of crystalline oxides and ceramic materials,^{1,3,5,6} and the response of these materials to ion bombardment and thermal annealing is being studied by means of ion channeling methods. In the present work, the response of two insulating materials, SrTiO_3 and CaTiO_3 , to heavy ion bombardment and their behavior during subsequent thermal annealing will be described. The results show that moderate doses of Pb ($\sim 1 \times 10^{15}/\text{cm}^2$) implanted at liquid nitrogen temperature are sufficient to render the near-surface region of single crystals of these titanates amorphous. Thermal annealing at temperatures ($< 500^\circ\text{C}$) that are quite low in comparison to the melting points of these materials causes the near-surface region to recrystallize epitaxially on the underlying single crystal substrate. For both SrTiO_3 and CaTiO_3 , the annealing process takes place by means of simple solid-phase epitaxy in which the amorphous-to-crystalline transformation occurs at a planar interface that moves toward the free surface of the material.

EXPERIMENTAL DETAILS

Single crystals of CaTiO_3 and SrTiO_3 were implanted with Pb (540 keV) to a dose of $1 \times 10^{15}/\text{cm}^2$ at liquid nitrogen temperature. CaTiO_3 has an orthorhombic structure and both low symmetry (a- or c-axis oriented, with $a \approx c$) and high symmetry (b-axis oriented) faces were implanted. SrTiO_3

[†]Research sponsored by the Division of Materials Sciences, U.S. Department of Energy under contract DE-AC05-84OR21400 with Martin Marietta Energy Systems, Inc.

has a cubic perovskite structure and crystals with a $\langle 100 \rangle$ orientation were used primarily, although limited studies were carried out on crystals with a $\langle 110 \rangle$ or $\langle 111 \rangle$ orientation. Following implantation, the crystals were annealed in air at temperatures in the range of 270–500°C for time periods ranging from a few minutes to many hours. The crystals were examined in the as-implanted state and after thermal annealing using 2 MeV Rutherford backscattering and ion channeling techniques. Selected crystals of CaTiO_3 were also examined by transmission electron microscopy (TEM).

Results Obtained for SrTiO_3

Figure 1a shows that the implantation of a modest dose of Pb (540 keV, $1 \times 10^{15}/\text{cm}^2$) into a (100) surface of SrTiO_3 at liquid nitrogen temperature is sufficient to turn the near-surface region amorphous. In Fig. 1a, the aligned yield in the implanted region reaches the random value in the Sr sublattice and the step in the aligned yield from the Ti sublattice is equivalent to the increase in the random value at the energy corresponding to the Ti leading edge. The depth of the amorphous region in Fig. 1a is ~ 1800 Å. Figure 1b shows that thermal annealing at 400°C for 30 min in air causes a significant reduction in the aligned yield from the implanted region demonstrating that the amorphous near surface layer has crystallized and is epitaxial with the underlying substrate. The aligned yield, however, is significantly higher than that in the virgin region showing that the recrystallized film is not defect free. Features in the aligned yield in both the Sr and Ti sublattices suggest that a dislocation network remains in the vicinity of the original amorphous/crystal interface after annealing. Positive identification of this structure is dependent on a detailed TEM examination.

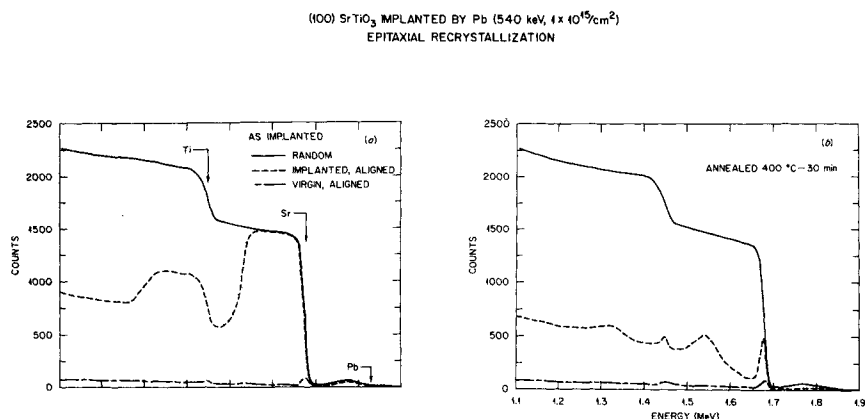


Fig. 1. Ion implantation and annealing of (100) SrTiO_3 . Ion channeling results are shown in 1a for the as-implanted state. Channeling results after annealing (400°C/30 min) are shown in 1b.